NANO LETTERS

pubs.acs.org/NanoLett

Single-Photon Generation by Electron Beams

Xesús Bendaña,[†] Albert Polman,[‡] and F. Javier García de Abajo*[,†]

[†]Instituto de Óptica—CSIC, Serrano 121, 28006 Madrid, Spain, and [‡]Center for Nanophotonics, FOM Institute for Atomic and Molecular Physics (AMOLF), Science Park 113, 1098 XG Amsterdam, The Netherlands

ABSTRACT We propose a drastically new method for generating single photons in a deterministic way by interaction of electron beams with optical waveguides. We find a single swift electron to produce a guided photon with large probability. The change in energy and propagation direction of the electron reveals the creation of a photon, with the photon energy directly read from the energy-loss spectrum or the beam displacement. Our study demonstrates the viability of deterministically creating single guided photons using electron beams with better than picosecond time uncertainty, thus opening a new avenue for making room temperature, heralded frequency-tunable sources affordable for scientific and commercial developments.

KEYWORDS Single-photon source, electron beam, optical fibers, quantum optics, EELS, cathodoluminescence

The impressive achievements during the last two decades in the design and demonstration of on-demand single-photon sources have been largely fueled by the perspective of applications in computing, cryptography, and metrology using quantum systems.[1−6] A device generating a single photon with close to 100% probability when pressing a button fulfills this ideal, which has been mainly pursued by creating a localized excitation (for example, in a trapped atom) that is made to decay along a well-prescribed direction.[7] The quantum nature of this type of light is unveiled by the observation of antibunching in the second-order intensity correlation of single-photon pulses.[8] However, only a few schemes exist that can produce single photons on demand with high degree of certainty, in contrast to classical sources such as an attenuated pulsed laser, which emits photons following Poissonian statistics. These so-called deterministic single-photon sources[9−16] rely on the ability to generate with a high degree of certainty an electronic excitation in a single atom, molecule, or quantum dot, the decay of which gives rise to the emission of one photon within a time window of the order of nanoseconds, as determined by the decay rate of the excitation.

Here, we propose a new method to generate single photons within a much shorter time window better than 1 ps with close to 100% probability. Our design intrinsically produces photons guided in an optical fiber or planar waveguide, thus maximizing the collection efficiency. It consists of exciting guided modes in an optical fiber by means of an electron beam. We present two different configurations in which detection of the electron after releasing energy and momentum to the photon reveals its creation. The scheme of Figure 1 illustrates one of these configurations, which we discuss first for tutorial purposes.

An electron is made to pass near a straight, thin optical fiber following a direction perpendicular to its axis of symmetry (Figure 1). The electron is accompanied by an evanescent electromagnetic field[17] that couples to the fiber and excites a guided photon with finite probability. The photon takes a wave vector $-\mathbf{k}_{\|}$ from the electron, which is recoiled with momentum $\hbar\mathbf{k}_{\|}$ in the opposite direction; this is schematically illustrated in Figure 1 by a change in the trajectory close to the fiber. The electron is subsequently energy-analyzed to resolve its energy loss by an amount equal to

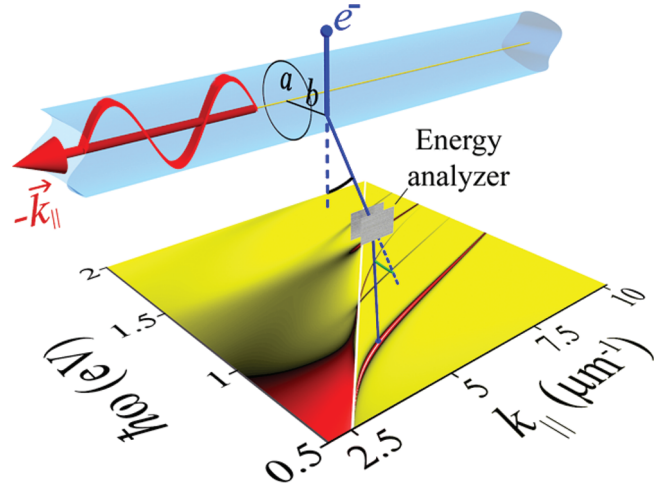

FIGURE 1. Single-photon generation by a fast electron. The electron (dark blue) passes near a thin optical fiber (light blue) in which it produces a guided photon (red) by coupling via its evanescent field. The energy $\hbar\omega$ and momentum $-\hbar\mathbf{k}_{\|}$ transferred from the electron to the photon give rise to deflection of the electron trajectory, which is recorded by an energy-angle analyzer. Detecting an electron with a combination of energy and momentum lying along a fiber guided band signals the generation of a single guided photon. This is shown in the lower color map, which represents the energy-momentum electron-probability distribution after a 25 keV electron passes at a distance $b - a = 10$ nm from the surface of a circular waveguide of radius $a = 200$ nm and refractive index $n = 2.45$. The light line ($\omega = k_{\|}c$) is indicated by the straight white line. Coupling of the electron to the two lowest order waveguide modes is clearly resolved in the region to the right of the light line.

* To whom correspondence should be addressed, J.G.deAbajo@csic.es.

Received for review: 10/2/2010
Published on Web: 00/00/0000

DOI: 10.1021/nl1034732 | *Nano Lett.* **XXXX,** *xxx,* 000–000

the photon energy $\hbar\omega$ (the analyzer is effectively deflecting the trajectory along a direction perpendicular to $\mathbf{k}_{||}$, as schematically shown in the figure). The probability that the electron undergoes an energy loss $\hbar\omega$ and transfers wave vector $\mathbf{k}_{||}$ is represented in the color plot of Figure 1 for 25 keV electrons passing at a distance of 10 nm from the surface of a cylindrical waveguide of radius $a = 200$ nm and refractive index $n = 2.45$. Like in the rest of the simulations reported in this work, photon generation intensities have been obtained by solving Maxwell's equations with the electron described as an external classical charge using a fast and rigorous two-dimensional version of the boundary element method, as reported elsewhere.[18] Energy-momentum transfers to the right of the light line ($k_{||} = \omega/c$, represented in white, where c is the speed of light) correspond to guided modes of the fiber; the coupling to the lowest-order fiber mode is clearly seen from its dispersion curve in Figure 1. The emission of far-field radiation light is indicated by the nonvanishing probability on the left of the light line. Figure 1 shows that the detection of an electron with a combination of energy and momentum corresponding to a waveguide mode reveals the generation of a photon characterized by the same energy and momentum. Consequently, this new method is not only energy but also mode selective.

Measurement of the transfer of energy and momentum from fast electrons to nanostructured materials is routinely performed using transmission electron microscopy (TEM) by collecting electron energy-loss spectra (EELS) and also in both TEM and secondary electron microscopy (SEM) to analyze the spatially resolved optical response encoded in the resulting cathodoluminescence emission.[17] In this context, electron beams have been shown to be capable of exciting propagating surface plasmons in metals and in particular in planar surfaces,[19,20] in nanowires,[21] in ridges,[22] and in grooves.[23] The mechanism involved in the excitation of guided photons in the present paper is similar to that of guided plasmon generation. The electromagnetic field of an electron beam can be separated into different components of frequency ω, each of which acts independently within the linear response regime. More precisely, the electric-field intensity as a function of distance d from the beam takes the form

$$|\mathrm{E}|^2 = \frac{4e^2\omega^2}{v^4\gamma^2}\left[\frac{1}{\gamma^2}K_0{}^2\left(\frac{\omega d}{v\gamma}\right) + K_1{}^2\left(\frac{\omega d}{v\gamma}\right)\right] \qquad (1)$$

where

$$\gamma = 1/\sqrt{1 - v^2/c^2}$$

is the Lorentz contraction factor, v is the electron velocity, and e is the electron charge. The modified Bessel functions K_m describe an exponential decay of the field intensity with d for $\omega d/v\gamma > 0.2$.[17] This decay reflects the fact that an electron moving with constant velocity vector cannot radiate in vacuum, and each ω component of the field is in fact an evanescent wave. Nonetheless, the latter couples to guided modes of the fiber in the configuration of Figure 1. The electric field intensity associated to these modes decays evanescently in the vacuum region outside the waveguide according to

$$|\mathrm{E}|^2 \propto K_m{}^2(k_\perp d') \qquad (2)$$

where d' is the distance to the waveguide center, m is the azimuthal quantum number (in particular, $m = 0$ for the fundamental, lowest-energy mode of Figure 1), and

$$k_\perp = \sqrt{(\omega/c)^2 - k_{||}{}^2}$$

The exponentially decaying Bessel functions in the fields of eqs 1 and 2 suggest that the electron−fiber coupling for the aloof configuration of Figure 1 must also decay exponentially with impact parameter b. This is confirmed from our simulations (not shown).

A quantitative assessment of the photon generation probability P is given in Figure 2 for the conditions of Figure 1. Figure 2a represents the probability for transfers of energy associated to a photon wavelength $\lambda = 1550$ nm as a function of the transferred wave vector $k_{||}$, normalized to the free-space light wave vector $k = 2\pi/\lambda$. The wide area to the left of $k_{||} = k$ corresponds to light emitted outside the waveguide, the integral of which yields the emission probability I_0, which is represented by a dashed curve in Figure 2b as a function of electron energy.

Integrating the photon generation probability over the fundamental waveguide mode (i.e., the feature just to the right of $k_{||} = k$ in Figure 2a), we find the solid curve in Figure 2b. Typically, one out of 10^3 electrons produces a guided photon within 1 eV of the photon energy range. For an electron beam current of 10 nA, this corresponds to a single-photon generation rate of 6×10^7 Hz over a 1 eV bandwidth. The relative intensity of guided and far-field photons is shown in Figure 2c; the ratio peaks around 25 keV electron energy (the evanescent field of slower electrons is too tighly concentrated near the beam, whereas faster electrons produce weaker interaction because they spend less time near the fiber).

In the geometry of Figure 1, the production of guided photons is relatively small. Furthermore, this configuration requires to determine both the energy and the angle of the electron, which can be very challenging for energetic beams (~25 keV) and small transferred photon wave vectors ($\sim 10^{-2}$ nm^{-1}), leading to small deflections of the trajectory (~20 μrad), requiring a well-collimated electron beam.

An alternative configuration for single-photon generation by swift electrons is presented in Figure 3. We consider an electron passing at a close distance from a curved waveguide with large radius of curvature R, as shown in Figure 3a. For

DOI: 10.1021/nl1034732 | *Nano Lett.* **XXXX,** *xxx,* 000−000

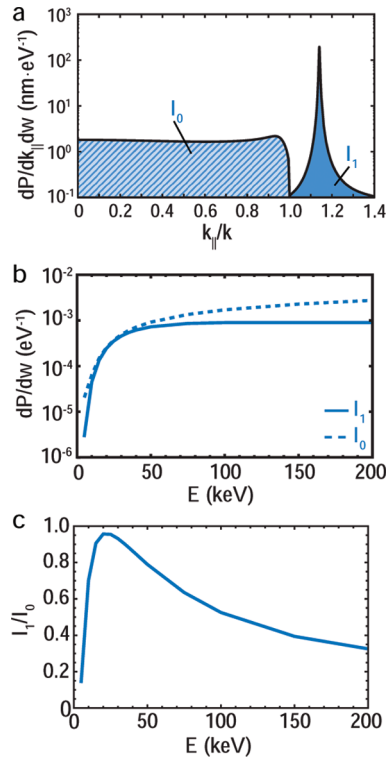

FIGURE 2. Photon generation probability. (a) Under the conditions of Figure 1, wave-vector dependence of the photon emission probability for a photon wavelength of 1550 nm, normalized per electronvolt of photon-energy range and inverse nanometer of wave-vector range. The wave-vector transfer $k_{||}$ is normalized to the free-space light wave vector k. (b) Intensity integrated over the radiative part of the spectrum (dashed curve, I_0, corresponding to the area for $k_{||} < k$ in (a)) and the fundamental mode of the waveguide (solid curve, I_1) as a function of electron-beam energy. (c) Ratio of the fundamental mode intensity I_1 to the radiative intensity I_0.

R much larger than the waveguide radius a, the electron trajectory is nearly parallel to the waveguide in the region of close proximity that contributes most to the photon emission. The analysis of this configuration can therefore be made by examining an electron moving parallel to a straight waveguide. The electron−surface distance varies adiabatically along the trajectory.

The inset of Figure 3b shows a dispersion diagram with the frequency-momentum dependence of the photon excitation probability for an electron moving parallel to a cylindrical silica fiber of radius $a = 300$ nm. The guided modes of the waveguide lie to the right of the light line (in white). Under the parallel-trajectory approximation, the electron can only transfer energy and momentum subject to the kinematical condition $\omega = k_{||}v$.[17] This relation is represented as a dashed blue line in the inset. Obviously, the electron moves slower than light in vacuum, so it can only excite guided modes of similar velocity in a process that resembles the emission of Cherenkov radiation for charges moving faster than light in a dielectric. The intersection of the electron dispersion and the fundamental mode of the waveguide is marked with a circle in the inset. The probability of generating a guided photon per unit of electron

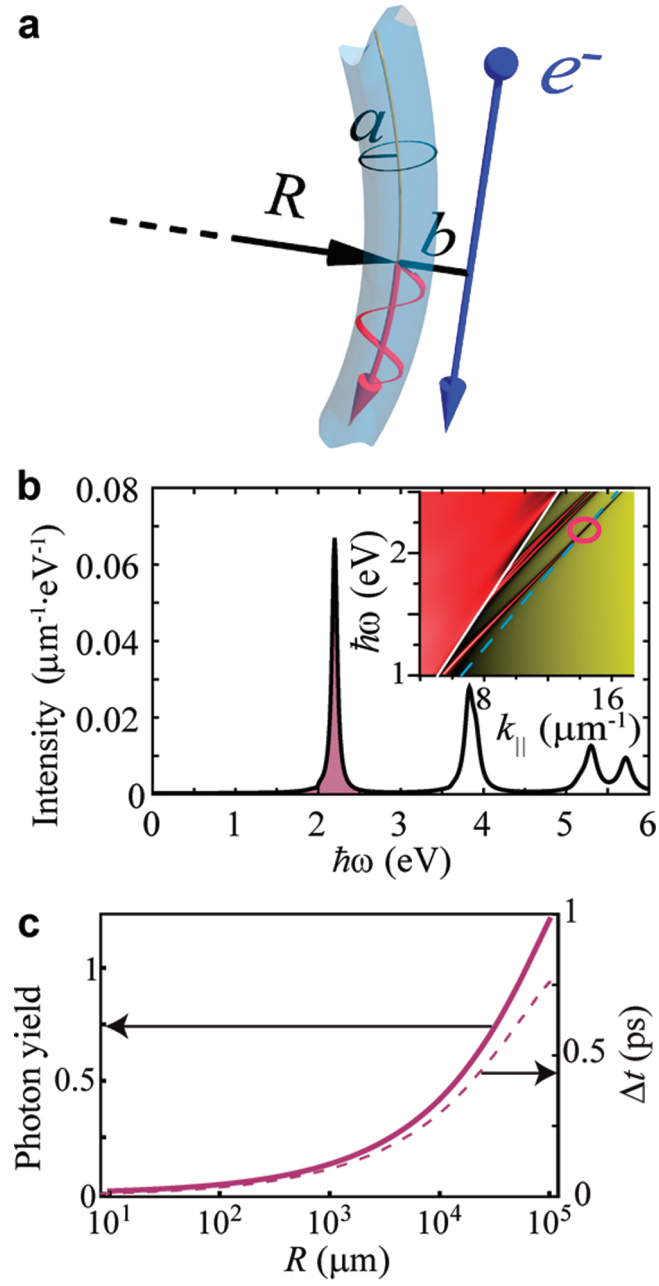

FIGURE 3. Photon generation by grazing electron beams. (a) Geometry under consideration, with an electron passing at a small distance from a curved waveguide compared to the curvature radius R. (b) Photon emission probability per unit of path length and photon-energy range for a 300 keV electron moving 10 nm outside the surface of a straight cylindrical silica waveguide of radius $a = 300$ nm (refractive index $n = 1.46$). The electron can only transfer excitations of energy and wave vector lying along the dashed line of the dispersion-plot inset. Guided modes in the inset are clearly visible to the right of the (white) light line. The main plot features sharp peaks corresponding to the excitation of different guided modes. (c) Photon generation yield under the conditions of (a) and (b) for a minimum electron−surface distance $b - a = 10$ nm. The emission probability, integrated in energy over the left-most peak of (b) and also along the trajectory, is given in units of photons per electron as a function of the curvature radius R (solid curve, left scale). The time interval Δt spent by each electron in the part of the trajectory where 90% of the photons are produced is shown by a dashed curve (right scale).

DOI: 10.1021/nl1034732 | *Nano Lett.* **XXXX,** *xxx,* 000–000

path length is shown in the main curve of Figure 3b as a function of photon energy for $b - a = 10$ nm. As expected, the emission vanishes everywhere except for conditions such that the electron and photon momenta are matching. In order to facilitate the representation of these peaks, a small imaginary part has been added to the dielectric function of the silica in the waveguide. The area under each peak is actually independent of the value of such an imaginary part when this is small. In fact, the peaks should have infinitesimally small width for the idealized parallel trajectory in lossless glass, although the waveguide curvature R can produce a finite width $\Delta\omega \sim v/(bR)^{1/2}$, as quantified from the number of optical cycles along which the electron−surface distance remains nearly unchanged during the electron trajectory. Likewise, nonresonant, spurious light emission can take place with a negligible relative probability $\sim \lambda/(bR)^{1/2}$ for $R \gg \lambda$.

The emission probability for the lowest-frequency mode (i.e., the area under the left peak of Figure 3b) is represented in Figure 3c as a function of curvature radius R (solid curves). This is calculated by integrating the emission rate per unit of path length along the electron straight-line trajectory; this rate is made to depend on the position along the trajectory through the instantaneous separation between the electron and the waveguide surface; the rate is actually calculated for each separation assuming a straight, parallel waveguide. The emission probability exhibits a fast increase with R, because the electron spends more time close to the waveguide for larger R.

The grazing beam configuration of Figure 3 yields remarkably high single-photon emission efficiencies per electron. An additional advantage is that it only requires measuring the electron energy and not its deflection angle after interaction with the fiber, in contrast to the scheme of Figure 1. Furthermore, the grazing configuration prevents any possible spurious emission that would arise in a true straight waveguide geometry from the intersection of the electron beam with other parts of the sample.

In practical terms, the narrow fiber can be patterned in a high-index material deposited on a flexible, lower-index substrate. For simplicity, we have considered a waveguide curved into a circular shape, but it would be equally useful to have a straight waveguide for a finite length flanked by curved segments. The electron-beam-fiber distance can be made as small as a fraction of a nanometer in currently available TEM setups,[24] so the distance of 10 nm considered in Figure 3 should be readily achievable with a compact electron-optics setup, specially considering that we do not need to raster the beam across the sample, as is done in electron microscopes. The energy resolution of these instruments is now ∼0.1 eV,[25] so that the energy of the fundamental mode and the separation between the first two modes (∼2 eV in Figure 3) can be easily resolved.

Alternatively, a low-energy beam of a few electronvolts can be produced using a cold emission gun and subsequently accelerated toward a diaphragm biased at a high voltage and situated close to the fiber, thus automatically producing a collimated beam of electrons having much larger kinetic energy along the direction of the acceleration stage. Electron spectrometry can then be performed after a deceleration stage following the fiber. This arrangement makes the separation of different guided modes easier because one has to resolve an energy loss of the same order of magnitude as the initial kinetic energy of the electrons.

If we aim at generating photons within the fundamental mode of Figure 3, any electron count within the wide spectral range of 1−3 eV should be counted as positive. Multiple photon generation by a single electron disqualifies as a positive count in this scheme, as the energy lost by the electron is clearly outside this range in that case. It should be noted that the photon energy can be tuned by varying the electron energy and, consequently, also the crossing point between the electron line and the fundamental mode in Figure 3b. The photon source is thus tunable.

With a low electron-beam current ∼1 nA, typical of TEM, and assuming a modest photon yield of 0.1 photons per electron (this corresponds to $R \approx 0.6$ mm in Figure 3c), one obtains $\sim 6 \times 10^8$ photons/s. Even higher photon rates can be achieved by increasing either the electron current, which is affordable for the large values of the beam-surface separation under consideration, or the fiber curvature R. We note that the time spent by each electron to produce a photon is also a relevant parameter, since this dictates the uncertainty in the time at which the photon is produced. Indeed, the time of arrival of the electron at the detector permits us to trace back the time of photon generation with an uncertainty determined by the interval spent by the electron at a close distance from the fiber, where photon emission probability builds up. The variation of that interval with R for 90% photon production is shown in Figure 3c (dashed curve, right scale). For $R = 0.6$ mm, as considered above, the time uncertainty is ∼0.1 ps, which is 5 orders of magnitude better than what has been currently achieved in other schemes of deterministic single-photon generation.[3]

Radiative losses in the curved fiber of Figure 3 can be estimated to be of the order of $(a/R)^2$.[26] Therefore, we have not considered them in our calculations, and they can be actually neglected for a curvature radius above 10 μm. Another factor of practical importance in the design of this type of photon source is the role played by roughness and defects in the waveguide. Similar criteria to those used in the design of integrated optical components and high Q cavities should be taken into consideration in order to minimize radiative losses below 1 dB levels. Additionally, this will reduce spurious photon emission due to interaction of the electromagnetic field of the electron with waveguide defects.

The present results can be straightforwardly extended to the generation of single plasmons in metallic waveguides, where electron-beam-induced plasmon generation has al-

DOI: 10.1021/nl1034732 | *Nano Lett.* **XXXX,** *xxx,* 000−000

ready been shown to be rather efficient.[27] In a practical configuration, one could use the same geometry as in Figure 3, with the dielectric fiber substituted by a plasmonic waveguide. The extension of the plasmon field outside the metal is similar to that of a guided mode in the dielectric fiber, and thus, one can essentially elaborate on the results of Figure 3 to design a single-plasmon source based on a plasmonic waveguide that follows a straight line over a distance of tens of micrometers. This type of source could be easily combined with other plasmonic elements for on-chip signal processing.

Generation of UV photons should be also possible using waveguides made of large band gap insulators. The basic requirement is to have a waveguide operating at the desired photon frequency with very low losses. The maximum photon energy that can be generated depends on the material band gap (e.g., up to ∼9 eV in a silica waveguide similar to that of Figure 3 with all dimensions scaled down by a factor of ∼4) and the ability to tailor such as a material into a curved waveguide.

It is important to stress that having the generated light within a fiber or planar waveguide suggests integrating this waveguide in a micro-optics circuit for making use of the single photons in the quantum applications noted above. Additionally, the extension of these ideas to nanostructured waveguides and multiple photon generation opens a new perspective for creating single photons (and perhaps also pairs of entangled photons) on demand with unique frequency-tunable, high yield, and ultrashort time uncertainty characteristics.

Acknowledgment. This work has been supported by the Spanish MICINN (MAT2007-66050 and Consolider Nano-Light.es). X.B. acknowledges a JAE scholarship from CSIC.

REFERENCES AND NOTES

(1) Lounis, B.; Orrit, M. *Rep. Prog. Phys.* **2005**, *68*, 1129–1179.
(2) Oxborrow, M.; Sinclair, A. G. *Contemp. Phys.* **2005**, *46*, 173–206.
(3) Scheel, S. *J. Mod. Opt.* **2009**, *56*, 141–160.
(4) Knill, E.; Laflamme, R.; Milburn, G. J. *Nature* **2001**, *409*, 46–52.
(5) Chen, S.; Chen, Y. A.; Strassel, T.; Yuan, Z. S.; Zhao, B.; Schmiedmayer, J.; Pan, J. W. *Phys. Rev. Lett.* **2006**, *97*, 173004.
(6) Kok, P.; Munro, W. J.; Nemoto, K.; Ralph, T. C.; Dowling, J. P.; Milburn, G. J. *Rev. Mod. Phys.* **2007**, *79*, 135–174.
(7) Claudon, J.; Bleuse, J.; Malik, N. S.; Bazin, M.; Jaffrennou, P.; Gregersen, N.; Sauvan, C.; Lalanne, P.; Gerard, J. M. *Nat. Photonics* **2010**, *4*, 174–177.
(8) Kimble, H. J.; Dagenais, M.; Mandel, L. *Phys. Rev. Lett.* **1977**, *39*, 691–695.
(9) Imamoglu, A.; Yamamoto, Y. *Phys. Rev. Lett.* **1994**, *72*, 210–213.
(10) Kim, J.; Benson, O.; Kan, H.; Yamamoto, Y. *Nature* **1999**, *397*, 500–503.
(11) Brunel, C.; Lounis, B.; Tamarat, P.; Orrit, M. *Phys. Rev. Lett.* **1999**, *83*, 2722–2725.
(12) Michler, P.; Kiraz, A.; Becher, C.; Schoenfeld, W. V.; Petroff, P. M.; Zhang, L. D.; Hu, E.; Imamoglu, A. *Science* **2000**, *290*, 2282.
(13) Lounis, B.; Moerner, W. E. *Nature* **2000**, *407*, 491–493.
(14) Yuan, Z. L.; Kardynal, B. E.; Stevenson, R. M.; Shields, A. J.; Lobo, C. J.; Cooper, K.; Beattie, N. S.; Ritchie, D. A.; Pepper, M. *Science* **2002**, *295*, 102–105.
(15) McKeever, J.; Boca, A.; Boozer, A. D.; Miller, R.; Buck, J. R.; Kuzmich, A.; Kimble, H. J. *Science* **2004**, *303*, 1992–1994.
(16) Mosley, P. J.; Lundeen, J. S.; Smith, B. J.; Wasylczyk, P.; U'Ren, A. B.; Silberhorn, C.; Walmsley, I. A. *Phys. Rev. Lett.* **2008**, *100*, 133601.
(17) García de Abajo, F. J. *Rev. Mod. Phys.* **2010**, *82*, 209–275.
(18) García de Abajo, F. J.; Howie, A. *Phys. Rev. B* **2002**, *65*, 115418.
(19) Bashevoy, M. V.; Jonsson, F.; Krasavin, A. V.; Zheludev, N. I.; Chen, Y.; Stockman, M. I. *Nano Lett.* **2006**, *6*, 1113–1115.
(20) van Wijngaarden, J. T.; Verhagen, E.; Polman, A.; Ross, C. E.; Lezec, H. J.; Atwater, H. A. *Appl. Phys. Lett.* **2006**, *88*, 221111.
(21) Vesseur, E. J. R.; de Waele, R.; Kuttge, M.; Polman, A. *Nano Lett.* **2007**, *7*, 2843–2846.
(22) Vesseur, E. J. R.; de Waele, R.; Lezec, H. J.; Atwater, H. A.; García de Abajo, F. J.; Polman, A. *Appl. Phys. Lett.* **2008**, *92*, No. 083110.
(23) Vesseur, E. J. R.; García de Abajo, F. J.; Polman, A. *Nano Lett.* **2009**, *9*, 3147–3150.
(24) Muller, D. A.; Tzou, Y.; Raj, R.; Silcox, J. *Nature* **1993**, *366*, 725–727.
(25) Lazar, S.; Botton, G. A.; Zandbergen, H. W. *Ultramicroscopy* **2006**, *106*, 1091–1103.
(26) Burton, R. S.; Schlesinger, T. E. *J. Lightwave Technol.* **1993**, *11*, 1965–1969.
(27) Cai, W.; Sainidou, R.; Xu, J.; Polman, A.; García de Abajo, F. J. *Nano Lett.* **2009**, *9*, 1176–1181.

DOI: 10.1021/nl1034732 | *Nano Lett.* **XXXX,** *xxx,* 000–000